

Tensile properties and thermal expansion of discontinuously reinforced aluminium composites at subambient temperatures

A. L. GEIGER*

Advanced Composite Materials, Corporation, Greer, SC 29651, USA

P. WELCH

Gencorp Aerojet, Electronic Systems Division, Azusa, CA 91702, USA

The effects of temperature on the mechanical properties and thermal expansion of two discontinuously reinforced aluminium composites have been determined over the range 300–100 K. Silicon carbide particulate-reinforced 2009 and 6092 aluminium alloys were studied by tensile testing, in which both longitudinal and transverse strains were recorded, and by thermal expansion measurements. The test results clearly show that cooling to 100 K induces plastic flow in the aluminium alloy matrices due to the thermal expansion difference between aluminium and silicon carbide. At very low temperatures, the linear region of the stress–strain curve is greatly reduced or eliminated and the Poisson's ratio, ν , increases. For the higher yield strength 2009 matrix composite, ν increases from a room-temperature value of 0.28 to 0.35 at 100 K. For the lower-strength 6029 matrix composite, ν increases from a room-temperature value of 0.33 to a value of 0.5 at 100 K. A Poisson's ratio of 0.5 is the value characteristic of plastic flow in an incompressible material. Changes in yield strength, Young's modulus and thermal expansion with decreasing temperature are also consistent with thermally induced plastic flow in the composite matrix.

1. Introduction

The properties of particulate-reinforced composites and their relationship to microstructure and to the properties of their constituents have been studied extensively at room temperature [1–3] and elevated temperatures [4, 5]. Relatively little work has been done on properties of these materials at subambient temperatures. In discontinuously reinforced aluminium (DRA), differences in thermal expansion between the ceramic reinforcement and the aluminium alloy matrix induce residual stresses in the composite as it is cooled from a high-temperature stress-free state [6–9]. The stress in the matrix at a distance R from the centre of a SiC particle can be expressed as $\sigma_m = -1.38 (R_i/R)^3 \Delta T$ [9] where R_i is the radius of the reinforcement particle and ΔT is the temperature drop (K). As ΔT increases (or R_i increases), tensile stress in the matrix increases. If ΔT is large enough, the matrix will be stressed beyond its yield point and will plastically deform. When a DRA sample is tension tested, cooling-stress-induced plastic deformation would be expected to reduce or eliminate the linear elastic region of the stress–strain curve and to increase Poisson's ratio from the range of 0.3 expected for elastic deformation [10, 11] towards 0.5, the value characteristic of plastic deformation [12]. Plastic deformation will affect composite thermal expansion

when the reinforcement phase is non-spherical. In the case of non-equiaxed ceramic reinforcement particles of low thermal expansion, aligned in the longitudinal direction, thermal expansion in the longitudinal direction will decrease and that in the transverse direction will increase with the onset of matrix plastic deformation, and the expansion–temperature curve will exhibit hysteresis [13].

In addition to inducing plastic deformation through thermal mismatch stresses, temperature reduction will affect the elastic and strain-hardening properties of the constituent phases of the composite. Room-temperature elastic properties of aluminium alloys and ceramics similar to the matrices and reinforcement of the composites studied in this work are given in Table I.

From 300–100 K, the temperature range examined in this work, Young's modulus of aluminium increases nearly linearly with decreasing temperature at a rate of -37.7 MPa K^{-1} [17]. Poisson's ratio for aluminium decreases approximately linearly with decreasing temperature at a rate of $5 \times 10^{-4} \text{ K}^{-1}$ [17]. No data on the temperature dependence of SiC elastic properties in this temperature are available. The strength of aluminium alloys generally increases with decreasing temperature. Fig. 1 shows the effect of temperature on the tensile yield and tensile ultimate strengths of ingot aluminium alloys similar to the

* Present address: Morganite Incorporated, Dunn, NC 28334, USA.

TABLE I Room-temperature properties of matrices and reinforcement used in DRA composites [14–16]

	2024-T6 ^a	6013-T6 ^b	SiC
Elastic modulus (GPa)	72.4	69.7	450
Poisson's ratio	0.33	0.33	0.19
CTE ^c (ppm/K)	22.9	23.4	3.4
TYS (MPa)	393	372	–
TUS (MPa)	476	406	–

^a Nominal composition (%) 4.4 Cu, 1.5 Mg, 0.6 Mn.

^b Nominal composition (%) 0.9 Cu, 0.75 Si, 0.95 Mg, 0.35 Mn.

^c Average CTE 0–100 °C.

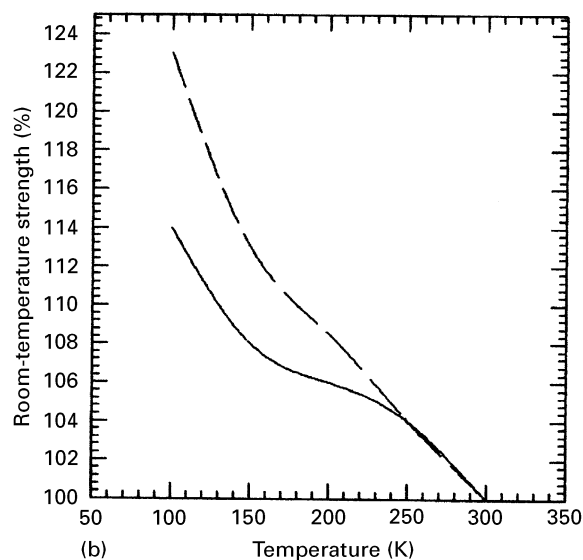
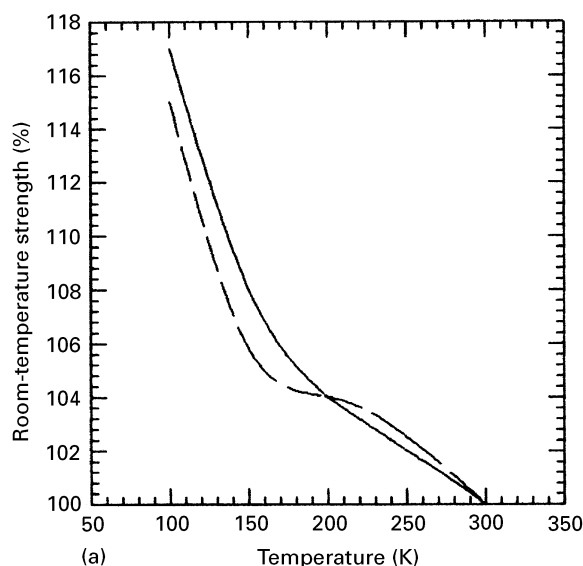


Figure 1 Temperature dependence of (—) tensile yield and (---) ultimate tensile strengths, on temperature for wrought aluminium alloys [18]: (a) 2024-T3, (b) 6061-T6.

matrix alloys used in the DRA composites studied in this work. The temperature dependence of coefficients of thermal expansion (CTEs) for aluminium and SiC are shown in Fig. 2.

In the present study, tensile properties and thermal expansion of two DRA composites with matrix alloys of differing strength have been measured from room

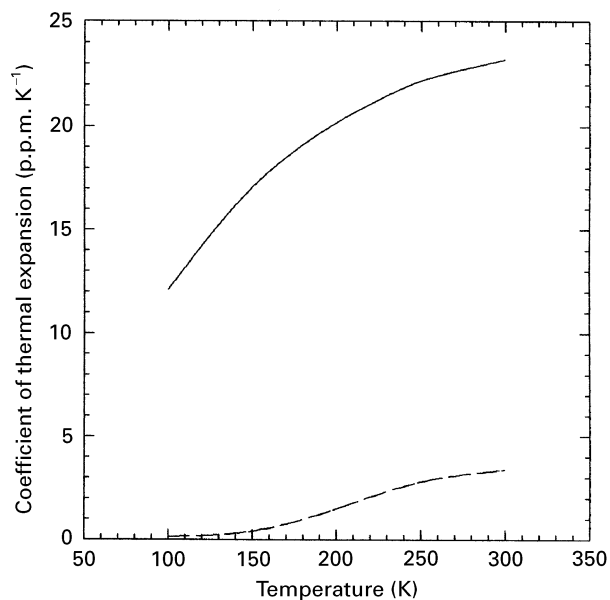


Figure 2 Temperature dependence of coefficients of thermal expansion for (—) aluminium and (---) silicon carbide [19].

TABLE II Composition of DRA materials

		2009/SiC/30 _p	6092/SiC/25 _p
Alloy matrix	Si (wt %)	0.5	0.7
	Fe (wt %)	0.1	0.1
	Cu (wt %)	3.3	0.7
	Mg (wt %)	0.8	1.0
	Al	Balance	Balance
SiC _p	Vol %	29.4	25.3
reinforcement	Mean diameter (μm)	2.2	3.3
Aspect ratio		~ 2:1	~ 2:1

TABLE III Heat treatment of DRA (T6P)

	2009/SiC/30 _p	6092/SiC/25 _p
Solution anneal	493 °C, 1 h	543 °C, 1 h
Quench	Cold water, < 5 s delay	Cold water, < 5 s delay
Artificial age	160 °C, 24 h	163 °C, 5 h

temperature to 100 K. The results are compared to composite model predictions.

2. Experimental procedure

Two DRA composites manufactured by Advanced Composite Materials Corporation, Greer, SC, were investigated in this study: 2009/SiC/30_p and 6092/SiC/25_p. These composites were made by blending aluminium alloy powders with particulate silicon carbide, vacuum hot-pressing to consolidate to 45.7 cm diameter, 295 kg cylindrical billets, and extruding the billets to round or rectangular bars. The compositions of the two DRA materials are given in Table II.

Extrusion causes the SiC_p reinforcement to become aligned with their long dimension parallel to the extrusion direction, making the composite properties anisotropic. The extruded bar was heat treated to T6P temper by the procedures given in Table III.

TABLE IV Specimen dimensions

Tensile (ASTM E8-93)	Overall length	203 mm
	Gauge length	51 mm
	Overall width	19 mm
	Gauge width	13 mm
	Thickness	3.2 mm
Thermal expansion	Length	51 mm
	Diameter	6.4 mm

Specimens for tensile and thermal expansion testing were machined from heat-treated bars at ACMC with their long axis parallel to the extrusion direction. The dimensions of the specimens are given in Table IV.

Tensile testing was performed at Delsen Testing Laboratories, Glendale, CA, in accordance with ASTM E8-93 using a crosshead speed of 1.3 mm min^{-1} . When tested at subambient temperatures, specimens were held at temperature for 10 min prior to testing. To monitor strain, a “T” gauge rosette (Measurements Group CEA-06-250UT-350, Raleigh, NC) was bonded to the gauge section of each specimen using Measurements Group AE-10 adhesive. Conventional tensile properties are computed from the engineering stress–strain curves. Yield stress is determined by the 0.2% offset method. Elastic modulus is determined by the slope of the chord of the stress–strain curve between 70 and 175 MPa (ASTM E111-8). Poisson’s ratio, ν , is determined as the absolute ratio of transverse to axial strain at 70 MPa.

Thermal expansion was measured by Ray E. Taylor and Hans Groot at the Thermophysical Properties Research Laboratory, Purdue University, using a dual push-rod dilatometer. The differential expansion between the sample and a standard reference material was measured as a function of temperature. Expansion of the specimen was computed from this differential expansion and the known expansion of the standard. Standard, calibrated reference materials were obtained from NIST.

TABLE V Tensile properties of DRA specimens at 300–100 K

Material	Temperature (K)	Ultimate strength (MPa)	Yield ^a strength (MPa)	Young’s ^b modulus (GPa)	Poisson’s ^c ratio	Strain to failure (%)
2009/SiC/30 _p	300	561	488	123	0.28	1.3
	250	544	489	122	0.29	0.9
	200	583	497	120	0.31	1.3
	150	608	514	119	0.35	1.3
	100	619	521	116	0.35	1.0
6092/SiC/25 _p	300	478	399	112	0.33	2.1
	250	471	394	108	0.35	1.5
	200	482	399	108	0.39	1.5
	150	510	397	107	0.41	2.2
	100	551	388	106	0.50	2.2

^a Offset = 0.2%.

^b Slope of chord between 70 MPa and 17 Pa stress.

^c Transverse strain/axial strain at 69 MPa stress.

3. Results and discussion

3.1. Tensile properties

Conventional tensile properties of the composites studied are given in Table V.

Typical engineering stress–strain curves for each composite at 300 and 100 K are shown in Figs 3 and 4. A linear elastic region is observed at 300 K, while no significant linear region exists at 100 K. This is consistent with the hypothesis that cooling stresses cause

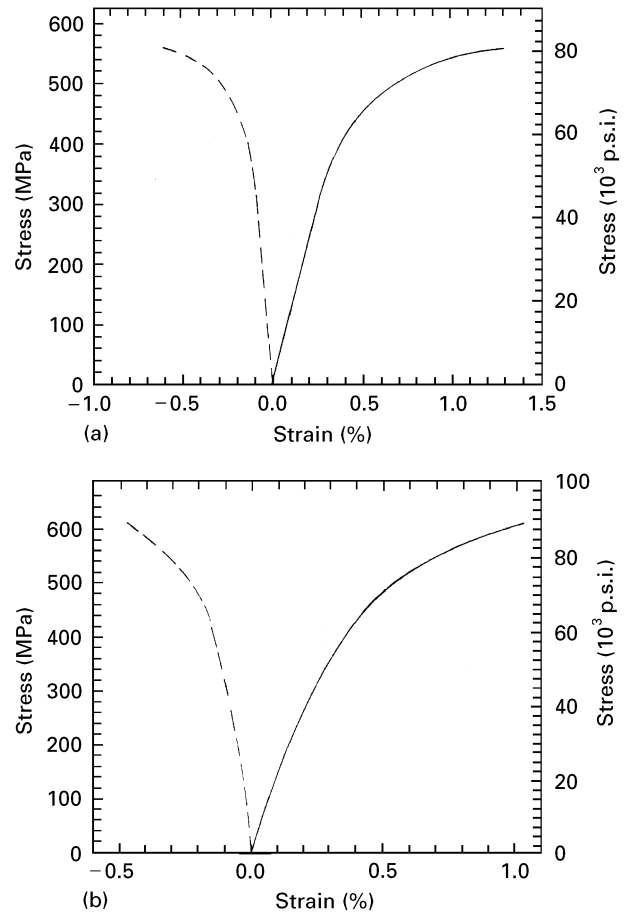


Figure 3 Engineering stress–strain curves for 2009/SiC/30_p-T6P: (—) longitudinal, (---) transverse; (a) 300 K (b) 100 K.

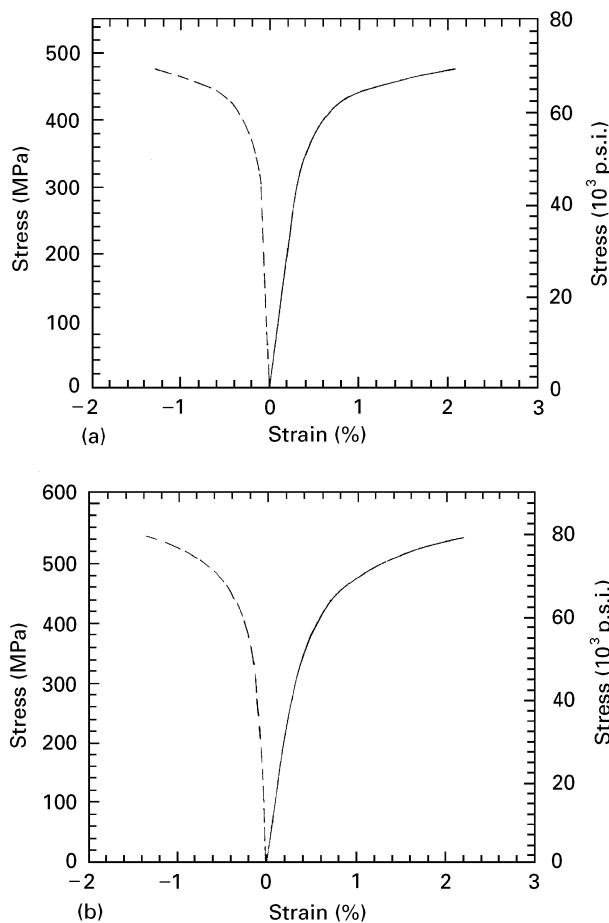


Figure 4 Engineering stress–strain curves for 6092/SiC/25_p-T6P: (—) longitudinal, (---) transverse; (a) 300 K (b) 100 K.

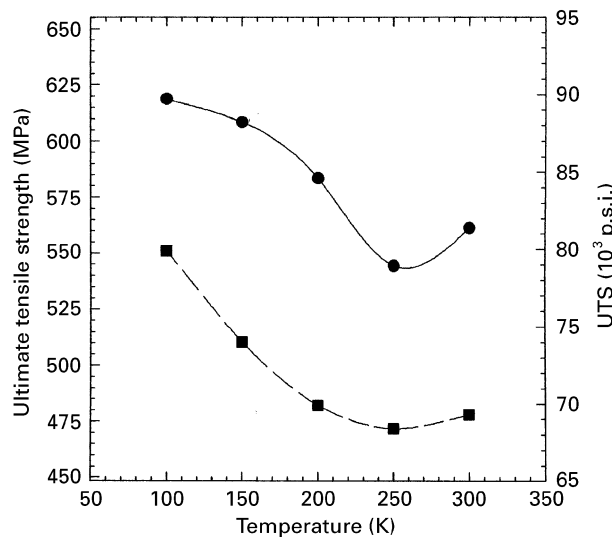


Figure 5 Temperature dependence of ultimate tensile strength for DRA: (●) 2009/SiC/30_p-T6P, (■) 6092/SiC/25_p-T6P.

matrix tensile stresses beyond their yield point at low temperatures. Additional tensile stress in the tension test causes immediate plastic flow in the matrix.

The temperature dependence of ultimate tensile strength (UTS) is shown in Fig. 5. UTS initially decreases with decreasing temperature, reaching a minimum at approximately 250 K. Below 250 K, UTS increases with decreasing temperature. The cause of

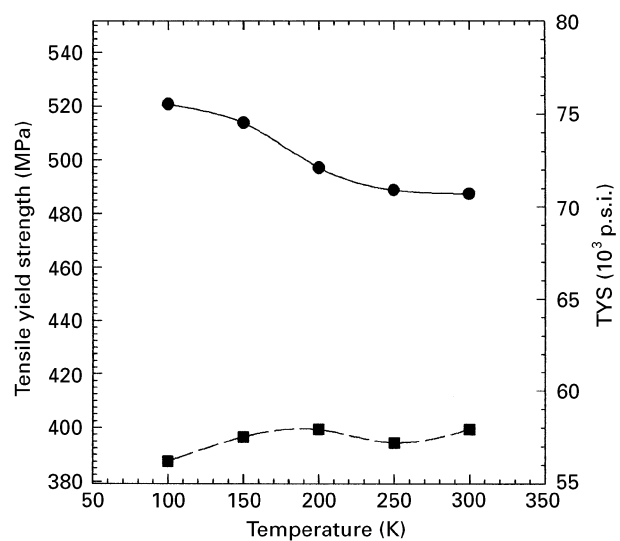


Figure 6 Temperature dependence of tensile yield strength for DRA: (●) 2009/SiC/30_p-T6P, (■) 6092/SiC/25_p-T6P.

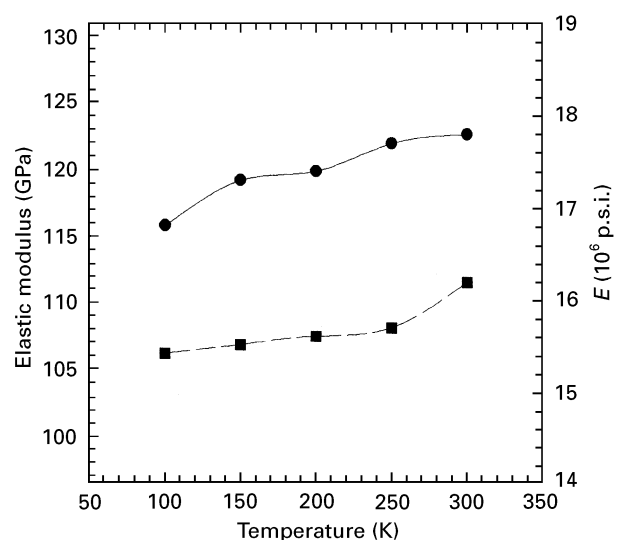


Figure 7 Temperature dependence of Young's modulus (chord modulus) for DRA: (●) 2009/SiC/30_p-T6P, (■) 6092/SiC/25_p-T6P.

the drop in strength from 300–250 K is not known. The increase in UTS from 250–100 K is similar to the increase seen in aluminium alloys. Over this temperature range, UTS of 2009/SiC/30_p-T6P increases 13.8%, compared to 12.1% for 2024-T3. For 6092/SiC/25_p-T6, UTS increases 15.5% compared to 18.3% for 6061-T6.

Tensile yield strength (TYS) versus temperature is shown in Fig. 6. TYS of 2009/SiC/30_p-T6P increases 6.8% as the temperature is reduced from 300 K to 100 K, much less than the 17% increase in TYS seen in 2024-T3. TYS of 6092/SiC/25_p-T6P exhibits a slight decrease with decreasing temperature. These results are also consistent with residual-stress-induced plastic deformation. Elastic deformation prior to plastic yielding decreases with decreasing temperature, so the 0.2% offset point will occur at lower stresses. The 6092 composite has a lower matrix yield stress and larger SiC_p reinforcement than the 2009 composite, so the reduction in TYS is more pronounced.

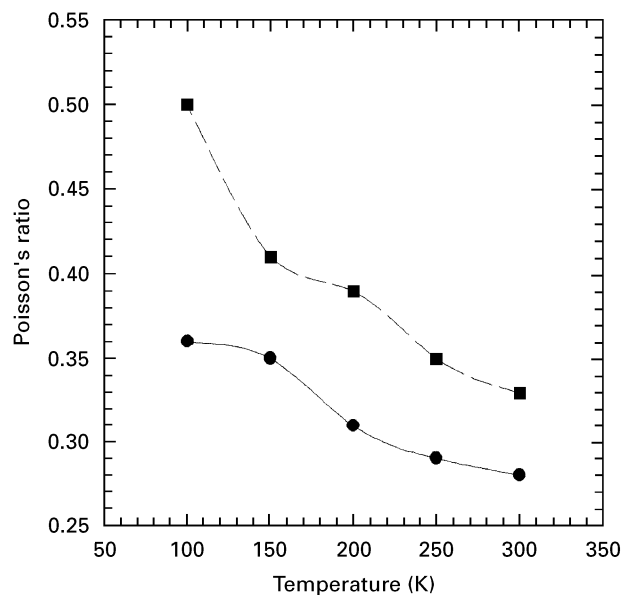


Figure 8 Temperature dependence of Poisson's ratio for DRA: (●) 2009/SiC/30_p-T6P, (■) 6092/SiC/25_p-T6P.

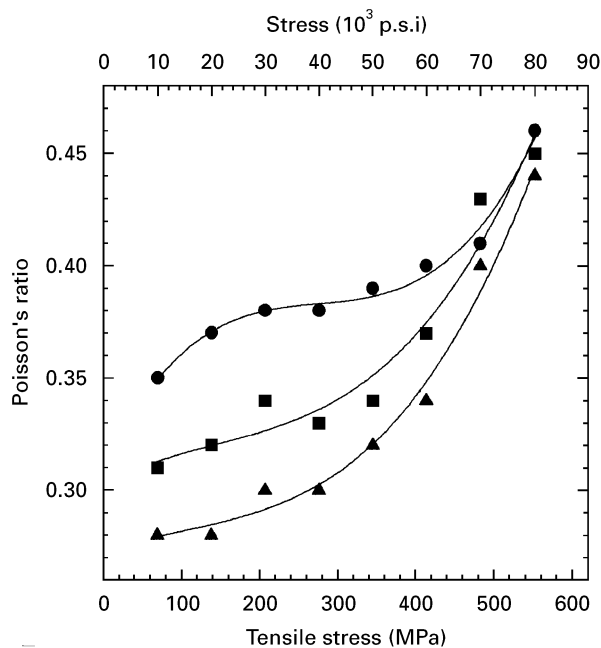


Figure 9 Poisson's ratio of 2009/SiC/30_p-T6P as a function of tensile stress at three different temperatures: (●) 100 K, (■) 200 K, (▲) 300 K.

Young's modulus, E , versus temperature is shown in Fig. 7. It is seen that E decreases slowly with decreasing temperature for both composites, opposite to the trend for aluminium. This also is caused by the deviation from linear elastic behaviour at low temperatures, which lowers the slope of the chord on the stress-strain curve used to compute E .

The temperature dependence of Poisson's ratio for each composite is shown in Fig. 8. The dependence of ν on tensile stress is shown at several temperatures in Figs 9 and 10. The low-stress ν for the 2009 matrix composite, which has a yield strength of 490 MPa, is 0.28 at room temperature, in good agreement with composite models based on elastic behaviour [10]. As temperature is decreased, low-stress ν increases to 0.36. This indicates that at low temperatures, some

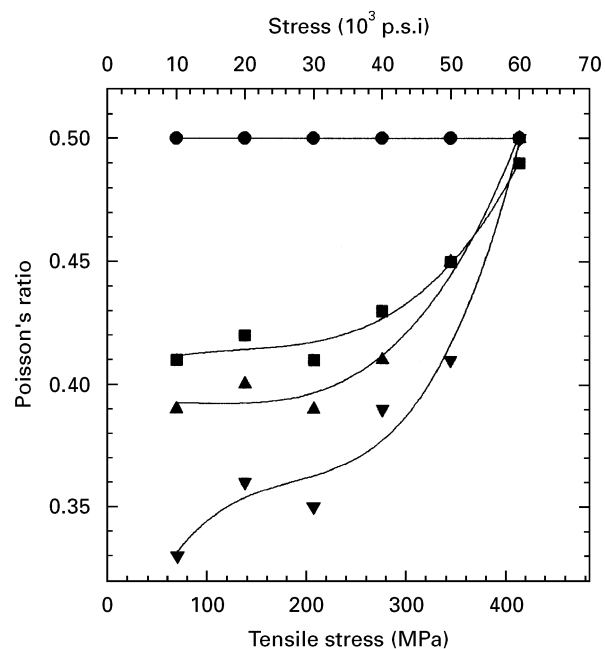


Figure 10 Poisson's ratio for 6092/SiC/25_p-T6P as a function of tensile stress at four temperatures: (●) 100 K, (■) 150 K, (▲) 200 K, (▼) 300 K.

plastic flow is occurring even at low tensile stresses. Poisson's ratio increases with increasing stress at all temperatures, reaching about 0.45 at 550 MPa, close to the value of 0.5 expected for plastic flow in an isotropic material. The stress dependence of ν for 2009/SiC/30_p-T6P at room temperature is similar to that observed by Singh and Lewandowski for a 2XXX/SiC/20_p composite [20].

For the 6092 matrix alloy, which has a yield strength of 400 MPa, the low-stress Poisson's ratio at room temperature is 0.33, above the value expected for elastic behaviour, indicating that some plastic deformation of the matrix has already occurred as a result of cooling following heat treatment. As the temperature is decreased, low-stress ν increases dramatically, particularly below 150 K. At 100 K, $\nu = 0.5$ for all values of tensile stress, showing that cooling stresses arising from differential contraction of the matrix and reinforcement have caused plastic deformation of the entire matrix.

3.2. Thermal expansion

Thermal expansion of the two composites is shown as a function of temperature in Fig. 11. Coefficients of thermal expansion are shown in Fig. 12. Between 300 and 220 K, the coefficient of thermal expansion decreases linearly with temperature. The 2009/SiC/30_p-T6P composite CTE decreases 17% over this range. Using literature values for the decrease in aluminium (9%) and silicon carbide (40%) CTEs as temperature decreases from 300 K to 220 K, a simple model for composite CTE [21] predicts a CTE drop of 14%, in reasonable agreement with the measured value. For the 6092/SiC/25_p-T6P composite, the observed CTE drop is 23%, while the model prediction is 13%. This deviation again may be due to plastic yielding in the lower-strength 6092 matrix.

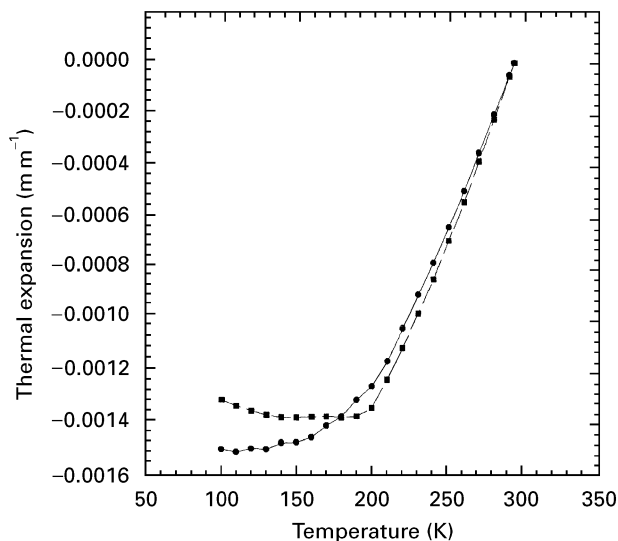


Figure 11 Thermal expansion of DRA: (●) 2009/SiC/30_p-T6P, (■) 6092/SiC/25_p-T6P.

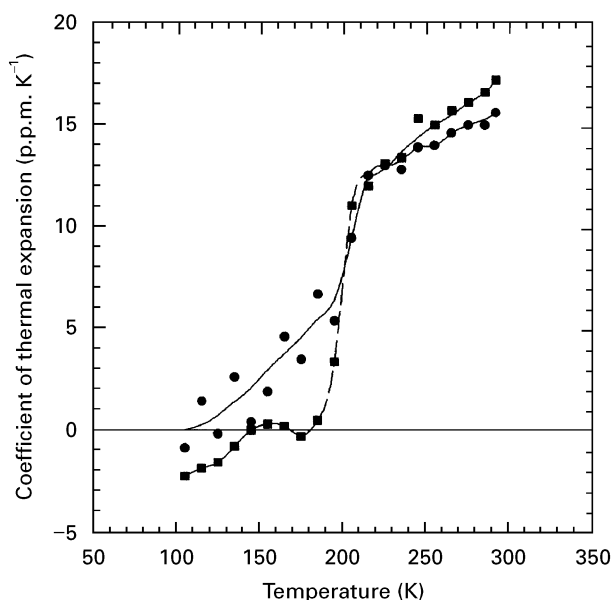


Figure 12 Coefficients of thermal expansion versus temperature for DRA: (●) 2009/SiC/30_p-T6P, (■) 6092/SiC/25_p-T6P.

Below 220 K, a large drop in CTE is observed for both composites. The 6092 composite shows virtually no change in length over the temperature range 200–100 K (CTE = 0). The 2009 matrix composite continues to contract over this range, but appears to reach a CTE of 0 at about 125 K. A reduction in longitudinal CTE is expected as plastic flow occurs [13], but not to the observed value of zero. DRA composites would be expected initially to exhibit elastic behaviour as the sample temperature is increased from 100 K, resulting in an expansion–temperature curve with pronounced hysteresis. Unfortunately, expansion on warming was not measured.

4. Conclusions

As the temperature is reduced from 300 K to 100 K, the mechanical and thermomechanical properties of discontinuously reinforced aluminium (DRA) are

increasingly controlled by thermally-induced plastic deformation of the aluminium alloy matrix caused by large differences in thermal expansion between the matrix and reinforcement phases. This has been shown by measurements of tensile properties and thermal expansion of two DRA composites over this temperature range. As test temperature is reduced from 300 K to 100 K, the following property changes are observed.

1. The linear region of the tensile–stress–strain curve decreases.
2. Tensile yield strength either decreases or increases much less than that of the equivalent matrix alloy.
3. Young's modulus decreases, opposite to the behaviour of aluminium alloys.
4. Poisson's ratio, ν , increases towards the value of 0.5, characteristic of plastic flow. The lower strength composite (6092/SiC/25_p-T6P) exhibits a greater increase in ν than the higher strength one (2009/SiC/30_p-T6P).
5. Thermal contraction becomes very small as the temperature is reduced below 200 K.

References

1. I. A. IBRAHIM, F. A. MOHAMED and E. J. LAVERNIA, *J. Mater. Sci.* **26** (1991) 1137.
2. A. MORTENSEN, J. A. CORNIE and M. C. FLEMINGS, *J. Metals* **40** (1988) 12.
3. A. L. GEIGER and J. A. WALKER, *J. Metals* **43** (1991) 8.
4. R. B. BHAGAT, M. F. AMATEAU, M. F. HOUSE, K. C. MEINERT and P. NISSON, *J. Compos. Mater.* **26** (1992) 1578.
5. F. A. MOHAMED, K. T. PARK and E. J. LAVERNIA, *Mater. Sci. Eng.* **A150** (1992) 21.
6. R. J. ARSENAULT and M. TAYA, *Acta Metall.* **35** (1987) 651.
7. J. K. LEE, Y. Y. EARMME, H. I. AARONSON and K. C. RUSSELL, *Metall. Trans.* **11A** (1980) 1837.
8. C. T. KIM, J. K. LEE and M. R. PLICHTA, *ibid.* **21A** (1990) 673.
9. Z. M. SUN, J. B. LI, Z. G. WANG and W. J. LI, *Acta Metall. Mater.* **40** (1992) 2961.
10. K. S. RAVICHANDRAN, *J. Am. Ceram. Soc.* **77** (1994) 1178.
11. M. LEI and H. LEDBETTER, *Metall. Trans.* **25A** (1994) 2832.
12. G. E. DIETER, *Mechanical Metallurgy*, 2nd edn (McGraw-Hill, New York, 1976).
13. K. WAKASHIMA, M. OTSUKA and S. UMEKAWA, *J. Compos. Mater.* **8** (1974) 391.
14. "Aluminium Standards and Data" (The Aluminium Association, Washington, DC, 1988).
15. "Alcoa Green Letter: Alcoa Aluminium Alloy 6013" (Aluminium Company of America, Pittsburgh, PA, 1987).
16. Battelle Memorial Institute, "Engineering Properties of Selected Ceramic Materials" (American Ceramic Society, Columbus, OH, 1966).
17. G. N. KAMM and G. A. ALERS, *J. Appl. Phys.* **35** (1964) 327.
18. "Military Handbook, Metallic Materials for Aerospace Vehicle Structures", MIL-HDBK-5G (United States Department of Defense, Washington, DC, 1994).
19. Y. S. TOULOUKIAN, R. K. KIRBY, R. E. TAYLOR, and P. D. DESAI (eds), "Thermophysical Properties of Matter", (Thermophysical Properties Research Center, W. Lafayette, IN, 1975).
20. P. E. SINGH and J. J. LEWANDOWSKI, *Metall. Trans.* **26A** (1995) 2911.
21. P. S. TURNER, *J. Res. Nat. Bur. Stand.* **37** (1946) 239.

Received 19 April
and accepted 17 September 1996